



## Adsorption of Cd (II) and Zn (II) from aqueous solutions using magnetic hydroxyapatite nanoparticles as adsorbents

Yuan Feng<sup>a,b</sup>, Ji-Lai Gong<sup>a,b,c,\*</sup>, Guang-Ming Zeng<sup>a,b</sup>, Qiu-Ya Niu<sup>a,b</sup>, Hui-Ying Zhang<sup>a,b</sup>, Cheng-Gang Niu<sup>a,b</sup>, Jiu-Hua Deng<sup>a,b</sup>, Ming Yan<sup>a,b</sup>

<sup>a</sup> College of Environmental Science and Engineering, Lushan South Road, Changsha, Hunan 410082, PR China

<sup>b</sup> Key Laboratory of Environmental Biology and Pollution Control, Hunan University, Ministry of Education, Changsha 410082, PR China

<sup>c</sup> State Key Laboratory of Chemo/Biosensing and Chemometrics, Hunan University, Changsha 410082, PR China

### ARTICLE INFO

#### Article history:

Received 10 February 2010

Received in revised form 22 May 2010

Accepted 26 May 2010

#### Keywords:

Metal ions

Magnetic adsorbents

Adsorption

Magnetic separation

### ABSTRACT

Magnetic hydroxyapatite nanoparticles (MNHAP) adsorbents were synthesized and were used for the removal of Cd<sup>2+</sup> and Zn<sup>2+</sup> from aqueous solutions. The properties of this magnetic adsorbent were characterized by scanning electron microscopy (SEM), energy dispersive analysis system of X-ray (EDAX), X-ray powder diffraction (XRD) analysis, zeta potential, BET surface area measurements and magnetization curves. Experiments were carried out to investigate the influence of different sorption parameters, such as contact time, initial concentration of metal ions, the dosage of MNHAP, pH value of the solutions and competitive adsorption behavior. Kinetic data are well fitted by a pseudo second-order model and the equilibrium data are analyzed by Langmuir model very well with high correlation coefficient. From the Langmuir isotherms, the maximum adsorption capacities of MNHAP adsorbents towards Cd<sup>2+</sup> and Zn<sup>2+</sup> are 1.964 and 2.151 mmol g<sup>-1</sup>, respectively. The results revealed that the most prominent advantage of the prepared MNHAP adsorbents consisted in their separation convenience compared to the other adsorbents.

© 2010 Elsevier B.V. All rights reserved.

### 1. Introduction

It is well known that heavy metals such as cadmium and zinc in environments pose a serious threat to plants, animals and even human beings because of their bioaccumulation, nonbiodegradable property and toxicity even at low concentrations [1]. In general, the pollution caused by heavy metals has detrimental effect on the environment all over the world. For example, a variety of toxic effects on aquatic organisms can be produced by endangering ecosystems; human health can be directly or indirectly influenced by multiple channels such as touching with skin, drinking water, and food chain. In addition, in agro-ecological environment, especially in soils, the phenomenon of heavy metals pollution is now quite common. Heavy metals cause great harm to the crop growth, yield and quality. So the removal of heavy metals, such as mercury, lead, zinc, copper, cadmium, and arsenic, from natural waters or soils has attracted considerable attention [2]. The conventional technologies for the removal of heavy metal ions from aqueous solution include chemical precipitation, ion exchange, reverse

osmosis, electrochemical treatment and adsorption [3]. Among the different treatments described above, adsorption technology is attractive due to its merits of efficiency, economy and simple operation [4]. The common adsorbents primarily include activated carbons, zeolites, clays, biomass and polymeric materials [5]. However, these adsorbents described above suffer from low adsorption capacities and separation inconvenience. Therefore, efforts are still needed to exploit new promising adsorbents.

In recent years, several studies have been performed to explore the application of mineral materials of environmental functions to dispose wastewater containing heavy metals. It is reported that zeolite [6,7], montmorillonite [8,9], rectorite [10,11], diatomite [12,13] and other mineral materials can treat wastewater by adsorption, ion exchange, precipitation and surface complexation because of their excellent surface characteristics and ion adsorption and exchange performance. As the mineral materials have the advantages of wide sources, low cost, simple process, easy use and no regeneration, mineral materials of novel environmental functions will have a great scientific, social and economic significance. It was reported that apatite-group minerals with special crystal chemistry characteristics would become the most promising mineral materials of environmental functions in the treatment of wastewater containing fluoride and heavy metals [14,15]. As a member of apatite mineral family, hydroxyapatite (Ca<sub>10</sub>(PO<sub>4</sub>)<sub>6</sub>(OH)<sub>2</sub>, HAP) is an ideal material for the disposal of long-

\* Corresponding author at: College of Environmental Science and Engineering, Lushan South Road, Changsha, Hunan 410082, PR China. Tel.: +86 731 88822829; fax: +86 731 88822829.

E-mail address: [jilaigong@gmail.com](mailto:jilaigong@gmail.com) (J.-L. Gong).

term contaminants because of its high sorption capacity for heavy metals, low water solubility, availability, low cost and high stability under oxidizing and reducing conditions [16]. The sorption mechanisms of the heavy metals are diverse and mainly include: ion exchange, dissolution/precipitation, and formation of surface complexes [17,18].

There are many reports on using HAP to remove a variety of metals. Recently, Zhou et al. [19] have synthesized a hydroxyapatite nanoparticle as adsorbent for the removal of copper ion. Dybowska et al. [20] have reported the natural and synthetic apatites for the removal of metals from aqueous solutions. Mignardi's group has studied the removal of copper and zinc from single- and binary-metal solutions using hydroxyapatite [21]. Smiciklas et al. [22] reported that HAP had high sorption capacity for  $\text{Cd}^{2+}$ ,  $\text{Zn}^{2+}$  and  $\text{Pb}^{2+}$ . They found that the maximum sorption capacity of HAP was 676.09, 67.55 and 37.53  $\text{mg g}^{-1}$  for  $\text{Pb}^{2+}$ ,  $\text{Cd}^{2+}$  and  $\text{Zn}^{2+}$  respectively. A comparative study of the adsorption of Cd, Zn and Co by calcite and HAP was performed by Cicerone and coworkers [23] using batch experiments. The results showed that both materials were effective for heavy metals retention, but HAP had better performance for water treatment due to its greater efficiency for the retention of Cd, Zn and Co. However, all the adsorbents based on HAP described above had the common drawback of inconvenience to separation.

Magnetic separation technology as an efficient, fast and economical method for separating magnetic materials has been widely used in textile, biology, and environmental protection [24–26]. The adsorbents combining magnetic separation technology with adsorption process have been widely used in environmental purification [27–29]. The main advantage of this technology is that it can dispose a mass of wastewater in a very short period of time and produce no contaminants.

In this study, we propose to synthesize magnetic hydroxyapatite nanoparticles (MNHAP) and explore the possibility of using MNHAP as adsorbents for the removal of  $\text{Cd}^{2+}$  and  $\text{Zn}^{2+}$  from aqueous solution. The MNHAP possess merits of high adsorption capacity of hydroxyapatite nanoparticles and separation convenience of magnetic materials. Furthermore, the removal of heavy metals from aqueous solution using MNHAP as adsorbents has never been reported in the literature. The MNHAP adsorbents were carefully characterized and the experimental parameters were also investigated in detail.

## 2. Materials and methods

### 2.1. Materials

$\text{Cd}(\text{NO}_3)_2$  and  $\text{Zn}(\text{NO}_3)_2$  standard samples were purchased from Institute for Environmental Protection in China.  $\text{FeCl}_2 \cdot 4\text{H}_2\text{O}$ ,  $\text{FeCl}_3 \cdot 6\text{H}_2\text{O}$ , ammonia (25%),  $\text{Ca}(\text{NO}_3)_2 \cdot 4\text{H}_2\text{O}$  and  $(\text{NH}_4)_2\text{HPO}_4$  were all analytical grade. All metal solutions were prepared from their nitrate salts (AR) and distilled water.

### 2.2. Synthesis of MNHAP

The synthesis of MNHAP was performed according to the literature previously reported with some modification [30]. Typically, appropriate amount of  $\text{FeCl}_2 \cdot 4\text{H}_2\text{O}$  (1.85 mmol) and  $\text{FeCl}_3 \cdot 6\text{H}_2\text{O}$  (3.7 mmol) was dissolved in 30 mL of deoxygenated water under a nitrogen atmosphere at room temperature, and then 10 mL of 25%  $\text{NH}_4\text{OH}$  solution was added to the resulting solution under vigorous mechanical stirring (300 rpm). A black precipitate was produced instantly. After 15 min, an amount of 50 mL of  $\text{Ca}(\text{NO}_3)_2 \cdot 4\text{H}_2\text{O}$  (33.7 mmol) and an amount of 50 mL of  $(\text{NH}_4)_2\text{HPO}_4$  (20 mmol) solutions whose pH were all adjusted to 11 were dropwise added

simultaneously to the obtained precipitate solution for 30 min with mechanical stirring. The resulting puce suspension was heated at 90 °C for 2 h and then the mixture was cooled to room temperature and aged for 12–24 h without stirring. The obtained precipitate was separated by a magnet, washed repeatedly with deionized water till neutrality, dried in the drying oven at 90 °C, and grinded with mortar. The final products were the prepared MNHAP adsorbents.

### 2.3. Adsorbent characterization

The size and morphology of the synthesized MNHAP was characterized by scanning electron microscopy analysis using a JSM-5600 LV microscope (JEO, Ltd., Japan). The sample composition and element contents were analyzed by energy dispersive analysis system of X-ray (EDAX) using a EDX-GENESIS (EDAX, Ltd., USA). The structure of the synthesized magnetic adsorbents was analyzed by X-ray powder diffraction (XRD) pattern recorded on a D/max 2550 X-ray Diffractometer (Rigaku, Japan) using  $\text{Cu K}\alpha$  radiation ( $\lambda = 0.1541 \text{ nm}$ ) in steps of  $0.05^\circ (2\theta) \text{ min}^{-1}$  from  $10^\circ$  to  $80^\circ (2\theta)$ . The Brunauer–Emmett–Teller (BET) specific surface area was determined by nitrogen adsorption–desorption at 77.30 K (Metallurgy ASAP 2010, USA). The zeta potential of MNHAP suspensions was measured using a Zeta Meter 3.0 (Zeta Meter Inc.) equipped with a microprocessor unit. The magnetic properties were characterized by magnetization curves using a HH-50 vibrating sample magnetometer in the condition of sensitivity 20 mV.

### 2.4. Adsorption experiments

The adsorption experiments of  $\text{Cd}^{2+}$  and  $\text{Zn}^{2+}$  were performed according to the batch method. The conical flasks containing 0.002 g adsorbent and 20.00 mL metal solution with the initial pH value  $5.0 \pm 0.1$  were placed on a constant temperature bath oscillator to vibrate at room temperature ( $25 \pm 1^\circ \text{C}$ ). After a period of time, the MNHAP were separated from the solutions using a permanent magnet and the initial and final metal concentrations were determined by a Perkin-Elmer Analyst 700 AAS.

#### 2.4.1. Effect of equilibration time

The effect of contact time on each metal sorption was studied in different time intervals ranging from 15 min to 2 days with the initial metal concentration of  $2 \times 10^{-3} \text{ mol L}^{-1}$ . After the completion of the reaction, conical flasks were taken out and the MNHAP adsorbents were separated followed by the determination of the residual metal concentrations.

#### 2.4.2. Effect of initial metal concentration

Sorption isotherms were obtained by equilibrating MNHAP with metal solutions of different initial concentrations  $10^{-4}$ – $10^{-2} \text{ mol L}^{-1}$  for 24 h. After separation, the final concentrations of metal in the solutions were measured.

#### 2.4.3. Effect of MNHAP amount

The suspensions containing different amount of MNHAP (from 0.05 to 0.5  $\text{g L}^{-1}$ ) and  $2 \times 10^{-3} \text{ mol L}^{-1}$  metal solution were placed on a constant temperature bath oscillator for 24 h. After separation, the residual metal concentrations in the solutions were measured.

#### 2.4.4. Effect of pH

Sorption behaviors of  $\text{Cd}^{2+}$  and  $\text{Zn}^{2+}$ , for the same initial concentration, equilibration time and adsorbent amount, were studied as a function of pH. The initial pH values were adjusted from 4 to 10, using  $\text{HNO}_3$  or  $\text{KOH}$  solution. After contacting for 24 h, the suspensions were separated and the residual metal concentrations were analyzed.

#### 2.4.5. Competitive adsorption of $\text{Cd}^{2+}$ and $\text{Zn}^{2+}$ in the total concentration changeless

In this part, our objective was to study the effect of two metal ions coexistence on the total adsorptive capacity of MNHAP. The experiment was conducted keeping the total concentration changeless  $2 \times 10^{-3} \text{ mol L}^{-1}$  and changed each metal ions concentration. The other conditions are the same as mentioned above.

#### 2.4.6. The effect on adsorption of $\text{Cd}^{2+}$ or $\text{Zn}^{2+}$ with the presence of $\text{Zn}^{2+}$ or $\text{Cd}^{2+}$

In this binary system, one metal ion was fixed to  $2 \times 10^{-3} \text{ mol L}^{-1}$ , the other one varied from  $10^{-4}$  to  $10^{-2} \text{ mol L}^{-1}$ . In order to make the comparison of sorption behavior more accurately, the initial concentrations selected in the range of  $10^{-4}$ – $10^{-2} \text{ mol L}^{-1}$  were consistent with that in single component system. The other conditions are the same as mentioned above.

### 2.5. Desorption experiments

In order to estimate the reversibility of  $\text{Cd}^{2+}$  and  $\text{Zn}^{2+}$  sorption, desorption experiments using solutions with different pH were performed. Firstly, MNHAP was loaded with  $\text{Cd}^{2+}$  or  $\text{Zn}^{2+}$  by equilibrating the adsorbent with  $2 \times 10^{-2} \text{ mol L}^{-1}$   $\text{Cd}^{2+}$  or  $\text{Zn}^{2+}$  solution. The resulting suspensions were separated and the final metal concentrations were determined. Subsequently, the solid residue was thoroughly washed several times with distilled water, and dried at  $90^\circ\text{C}$ . Secondly, amount of 0.1000 g of the obtained adsorbents was added into 20 mL of four kinds of eluants including EDTA, HCl,  $\text{Ca}(\text{NO}_3)_2$  and NaOH respectively at room temperature ( $25 \pm 1^\circ\text{C}$ ) under vibration conditions for 24 h. After the completion of the reaction, the metal concentration in each eluant was measured.

## 3. Results and discussion

### 3.1. Properties of prepared magnetic adsorbents

The scanning electron microscope (SEM) micrograph of MNHAP is shown in Fig. 1. The result showed that the synthesized MNHAP were spherical shape with the diameter of about 28 nm and were aggregated with many nanoparticles, which resulted in a rough surface and porous structure. Fig. 2 shows the EDAX spectra of MNHAP adsorbents before and after loaded with  $\text{Cd}^{2+}$  and  $\text{Zn}^{2+}$  respectively. The Ca/P molar ratio of the MNHAP adsorbents is 1.65, which is less than the ideal stoichiometric apatite (1.67). Table 1 indicates the presence of iron and oxygen in addition to major constituents – calcium and phosphorous in sample of MNHAP adsorbent. Comparing the spectra of the MNHAP loaded with  $\text{Cd}^{2+}$  and  $\text{Zn}^{2+}$  with that of unloaded one, the cadmium peak and zinc peak could be observed. It was suggested that heavy metals including  $\text{Cd}^{2+}$  and  $\text{Zn}^{2+}$  had been adsorbed on the surface of MNHAP successfully. Moreover, after loading with heavy metal, a distinct decrease of calcium peak intensity could be found. This phenomenon might be derived from the participation of certain degree of interchange in the  $\text{Cd}^{2+}$  and  $\text{Zn}^{2+}$  adsorption. In addition, the diminution of the phosphate peak could be observed after adsorption (shown in Fig. 2b and c). The reason may be caused by the fact that the adsorption of heavy metal such as cadmium or zinc on the surface of MNHAP adsorbent lead-

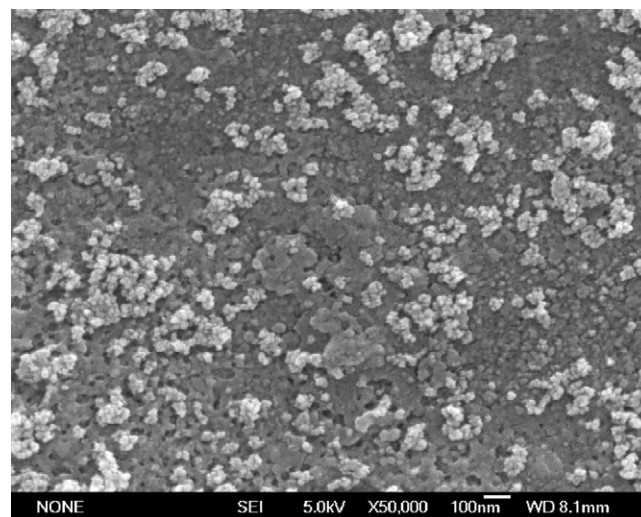


Fig. 1. SEM micrograph of the synthesized MNHAP adsorbents.

ing to the increase of total amount of MNHAP adsorbent and the decrease of phosphate proportion.

The BET surface area of MNHAP adsorbent was  $142.5 \text{ m}^2 \text{ g}^{-1}$ , which was higher than that of HAP previously reported [18,23,31–33]. Fig. 3 shows XRD pattern of the prepared MNHAP adsorbent. It was observed that the principal components of MNHAP adsorbent included hydroxyapatite (HAP), magnetite ( $\text{Fe}_3\text{O}_4$ ) and maghemite ( $\text{Fe}_2\text{O}_3$ ). Among them, the magnetite and maghemite were magnetic.

The room-temperature magnetization curve of the MNHAP (Fig. S1) showed that the saturation magnetization is  $59.4 \text{ emu g}^{-1}$  indicating a relatively strong magnetic response to a magnetic field. Saturation magnetization, used to measure the maximum magnetic strength, is a crucial parameter for successful magnetic separation. Ma et al. [34] found that a saturation value of  $16.3 \text{ emu g}^{-1}$  was sufficient for magnetic separation with a conventional magnet. Thus, the saturation magnetization value of MNHAP was high enough for magnetic separation. Fig. S2 shows that MNHAP adsorbent suspensions in aqueous solution can be separated from the solutions by an external magnetic field conveniently. Therefore, the MNHAP can be used as magnetic adsorbents for the removal of  $\text{Cd}^{2+}$  and  $\text{Zn}^{2+}$  from aqueous solution.

### 3.2. Sorption study

#### 3.2.1. Sorption kinetics

The results of sorption studies, carried out as a function of contact time, for  $\text{Cd}^{2+}$  and  $\text{Zn}^{2+}$  were presented in Fig. 4. It suggested that the removal of  $\text{Cd}^{2+}$  and  $\text{Zn}^{2+}$  by the MNHAP adsorbents took place in two distinct steps: a relatively quick phase (first 2 h), followed by a slow increase until the equilibrium was reached. The necessary time to reach the equilibrium was about 24 h. Though there was a slight increase of adsorption quantity after 24 h, it did not bring any remarkable effect, so a contact time of 24 h was chosen for further experiments.

Table 1  
The chemical composition of MNHAP before and after loaded with  $\text{Cd}^{2+}$  and  $\text{Zn}^{2+}$ .

Substance	Ca (At %)	P (At %)	O (At %)	Fe (At %)	Cd (At %)	Zn (At %)
MNHAP	24.49	14.81	45.41	15.28	0	0
MNHAP loaded with Cd	20.13	14.77	45.62	14.67	4.80	0
MNHAP loaded with Zn	18.29	14.69	45.03	15.44	0	6.54

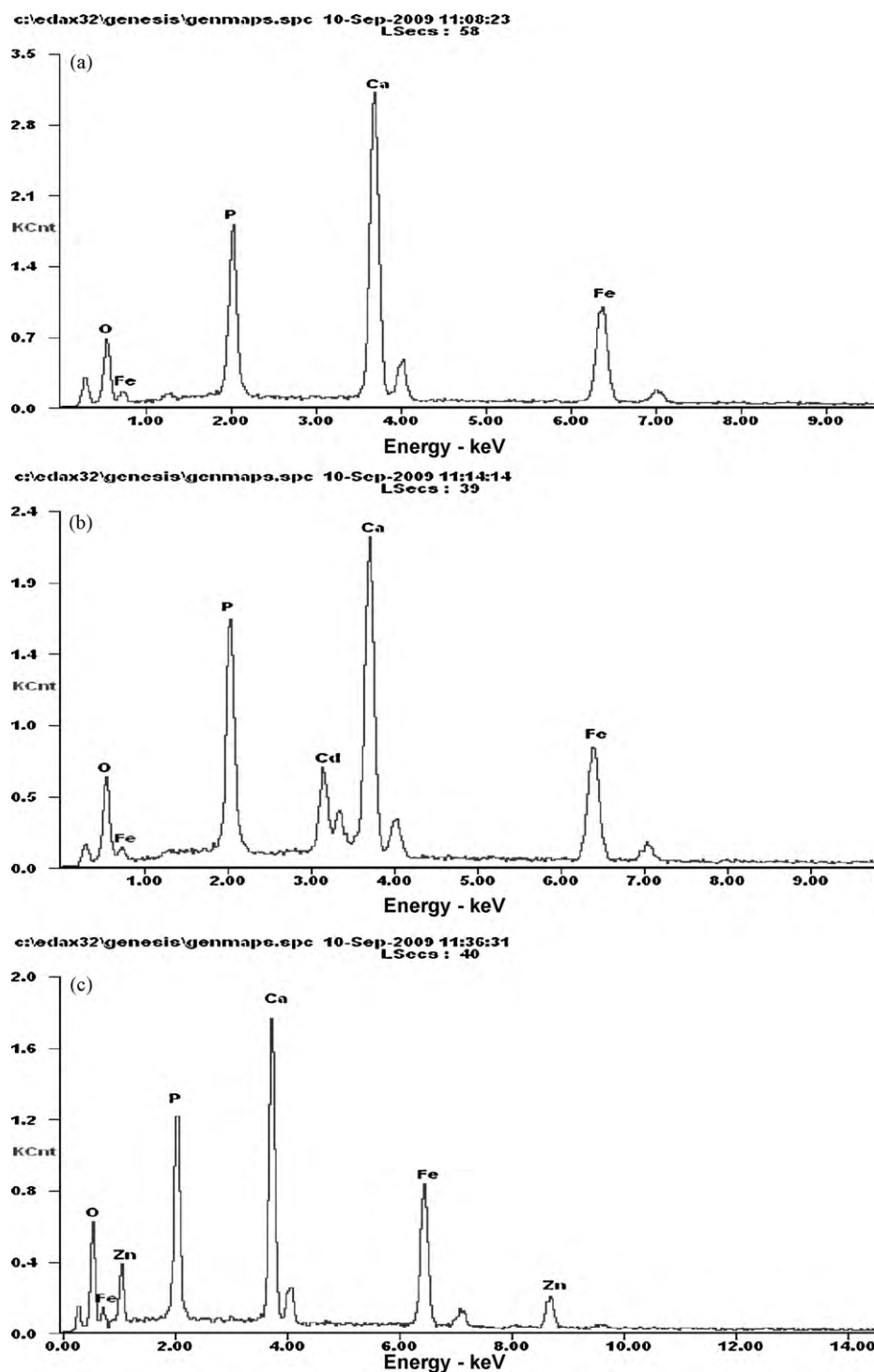


Fig. 2. EDAX spectra of the magnetic adsorbents (a) MNHAP (b) MNHAP loaded with Cd<sup>2+</sup> and (c) MNHAP loaded with Zn<sup>2+</sup>.

In order to determine the rate constants, the pseudo-second-order kinetic model was applied to our experimental result. The linear form of pseudo second-order model can be expressed as Eq. (1):

$$\frac{t}{q_t} = \frac{1}{kq_e^2} + \frac{t}{q_e} \quad (1)$$

where  $q_e$  and  $q_t$  are the amounts of metal ions adsorbed at equilibrium and any time  $t$  ( $\text{mmol g}^{-1}$ ), respectively,  $k$  is the rate constant of pseudo-second-order kinetics ( $\text{g mmol}^{-1} \text{h}^{-1}$ ). The second-order rate constant  $k$  and  $q_e$  can be determined from

the intercept and slope of the plot obtained by plotting  $t/q_t$  versus  $t$ .

Table S1 lists the results of applying pseudo second-order model to our experiment data. A linear relationship with high correlation coefficient ( $R^2 = 0.9999$  for both Cd<sup>2+</sup> and Zn<sup>2+</sup>) between  $t/q_t$  and  $t$  was obtained which indicated the applicability of the pseudo second-order model to describe the adsorption process. In previous papers, the pseudo-second-order kinetic model was found to be appropriate for describing kinetics of metal sorption by different apatite materials, such as: Cr<sup>3+</sup> by animal bones [35], Cd<sup>2+</sup> by bone char [36], Pb<sup>2+</sup> by soil

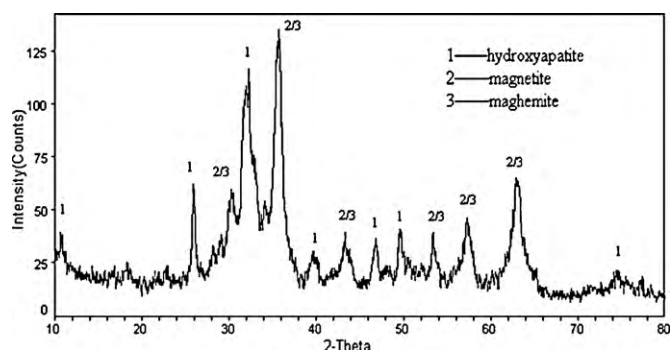


Fig. 3. XRD pattern of the MNHAP.

amended with HAP [37], and uranium by low-cost rock phosphate [38].

### 3.2.2. Sorption isotherms

In order to determine the sorption capacity of MNHAP adsorbents towards examined metal ions, sorption studies over a large initial concentration range from  $10^{-4}$  to  $10^{-2}$  mol L $^{-1}$  were carried out. The maximum adsorption capacities of the MNHAP adsorbent for heavy metals were evaluated using the adsorption isotherms. The Langmuir adsorption isotherm was employed to describe the adsorption behavior in the present study and the results are shown in Fig. 5. The linear form of Langmuir isotherm equation is given by Eq. (2):

$$\frac{1}{q_e} = \frac{1}{q_m b C_e} + \frac{1}{q_m} \quad (2)$$

where  $q_e$  and  $C_e$  are the equilibrium concentrations of metal ions in the adsorbed (mol g $^{-1}$ ) and liquid phases (mol L $^{-1}$ ), respectively,  $q_m$  is the maximum adsorption capacity (mol g $^{-1}$ ), and  $b$  is Langmuir constant which is related to the energy of adsorption (L mol $^{-1}$ ). The constants  $b$  and  $q_m$  can be determined from the slope and intercept of the linear plot  $1/q_e$  versus  $1/C_e$ . The results showed that the values of correlation coefficient for the adsorption of Cd $^{2+}$  and Zn $^{2+}$  onto MNHAP adsorbents were 0.9999 and 0.9950 respectively, which demonstrated the good fitting of experimental data by this model. The Langmuir constant for Cd $^{2+}$  and Zn $^{2+}$  was  $2.112 \times 10^3$  and  $1.957 \times 10^3$  L mol $^{-1}$  respectively, which illustrated that the MNHAP had better adsorption affinity for Cd $^{2+}$  than for Zn $^{2+}$  since the Langmuir constant was proportional to the binding energy. The  $q_m$  values for the adsorption of Cd $^{2+}$  and Zn $^{2+}$  by the MNHAP were 1.964 and 2.151 mmol g $^{-1}$ , respectively. Comparing with the maximum adsorption capacity of HAP reported by previous studies, Xu

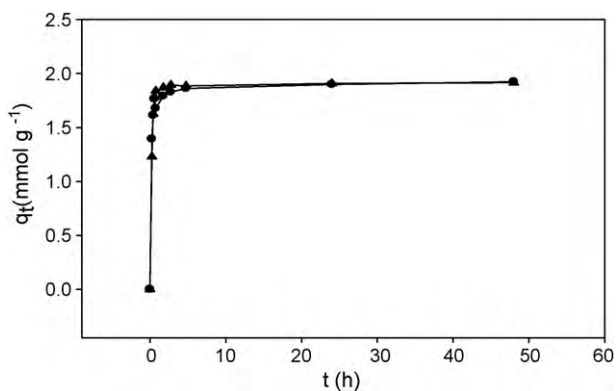


Fig. 4. Adsorption kinetic curves of heavy metals by MNHAP adsorbents at pH  $5.0 \pm 0.1$  and  $T = 25 \pm 1$  °C. (●) Cd $^{2+}$  and (▲) Zn $^{2+}$ . Initial concentration of heavy metals: Cd $^{2+}$   $2 \times 10^{-3}$  mol L $^{-1}$  and Zn $^{2+}$   $2 \times 10^{-3}$  mol L $^{-1}$ , MNHAP = 1 g L $^{-1}$ .

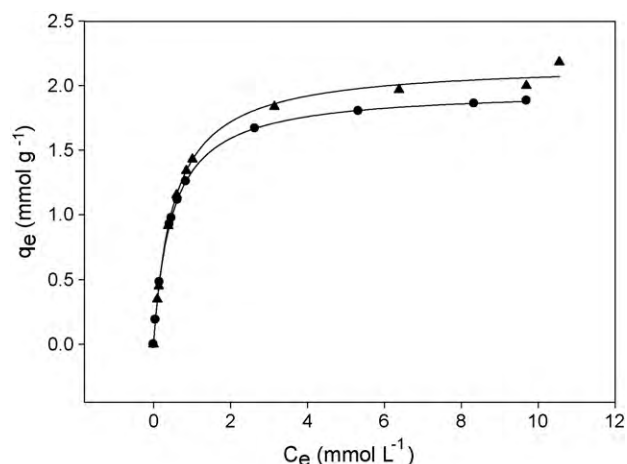


Fig. 5. Adsorption isotherm of heavy metals by MNHAP adsorbents at pH  $5.0 \pm 0.1$  and  $T = 25 \pm 1$  °C. (●) Cd $^{2+}$  and (▲) Zn $^{2+}$ .

et al. [18] reported that the maximum adsorption capacity of HAP for Cd $^{2+}$  and Zn $^{2+}$  was 0.592 and 0.568 mmol g $^{-1}$ , respectively. Smiciklas et al. [22] reported that the maximum adsorption capacity of HAP for Cd $^{2+}$  and Zn $^{2+}$  was 0.601 and 0.574 mmol g $^{-1}$ , respectively, the prepared MNHAP possessed an absolute advantage with much higher adsorption capacity which may be derived from its larger BET specific surface area. In addition, the control experiments were conducted in our measurements. The results showed that the removal amount of heavy metals by the pure iron oxides was only about 0.114 and 0.177 mmol g $^{-1}$  for Cd $^{2+}$  and Zn $^{2+}$ , respectively, and the amount of metals adsorbed by pure apatite was 1.137 and 0.993 mmol g $^{-1}$  for Cd $^{2+}$  and Zn $^{2+}$ , respectively.

### 3.2.3. Effect of MNHAP amount

The relationship between MNHAP amount and the heavy metals adsorption quantities was shown in Fig. 6. The results showed that the amount of heavy metals adsorbed increased rapidly with the increasing of MNHAP amount at the beginning. When the amount of the MNHAP was 0.1 g L $^{-1}$ , the adsorption amount reached maximum followed by a decrease of the adsorption amount as the MNHAP dosage increased. The reason for this phenomenon was that, for a fixed initial concentration of heavy metals, the amount of metal retained by gram of MNHAP increased with the amount of MNHAP (increases the no. of sites available) before the max-

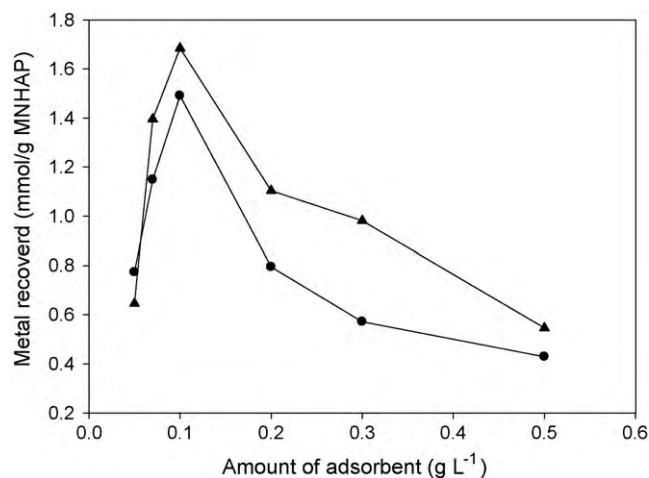


Fig. 6. The relationship between MNHAP dosage and heavy metals adsorbed on MNHAP adsorbents, (●) Cd $^{2+}$  and (▲) Zn $^{2+}$ .

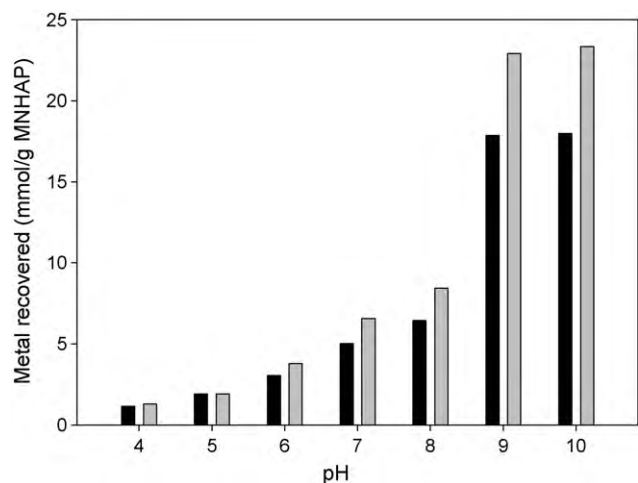


Fig. 7. The effect of initial pH values on the amount of the heavy metals adsorbed on MNHAP adsorbents, grey color represents Cd<sup>2+</sup>, black color represents Zn<sup>2+</sup>.

imum (conditions of saturation), and when more MNHAP were added after the maximum (the retention is almost total), the same cations were distributed on greater amount of surface and therefore resulted in the reduction of adsorption amount on unit mass adsorbent. Since the adsorption capacity reached maximum at the point of 0.1 g L<sup>-1</sup>, this dosage was chosen in the following experiments.

### 3.2.4. Effect of pH

The influence of initial pH on adsorption amount was studied in the range of 4–10. The relationship between the initial pH values and the quantities of heavy metals adsorbed on MNHAP adsorbents was presented in Fig. 7 which showed that the metal ions adsorbed increased as pH increased. It was noticed that when the pH value is higher than 8, the adsorption amount increased dramatically, which was attributed to the fact that heavy metal ions started to precipitate leading to the reduction of the metal ions in the aqueous solution at higher pH value. Fig. S3 shows the XRD patterns of the precipitation of metal complexes. It was observed that there were two ingredients in the cadmium complexes including Cd(OH)<sub>2</sub> and CdCO<sub>3</sub>. Two other ingredients such as Zn(OH)<sub>2</sub> and ZnO existed in the precipitation of zinc complexes. Similar results were obtained when divalent cations were removed by hydroxyapatite in the previous literature [22]. From the data of the zeta potential (Fig. S4), we knew that the charge sign on the surface of MNHAP adsorbents was negative in the entire examined range which provided a strong theoretical basis for the existence of electrostatic attraction between the MNHAP surface and the metal ions. Also we could observe that negative charge on the MNHAP surface reduced gradually when pH value is greater than 5, while the adsorption amount increased little by little. The results showed that some other sorption mechanism should be in existence during the adsorption process except for electrostatic attraction. The lowering of the Ca<sup>2+</sup> peak intensity of MNHAP adsorbents after loading with Cd<sup>2+</sup> and Zn<sup>2+</sup> in the EDAX spectra (see Fig. 2) indicated the participation of certain degree of interchange in the Cd<sup>2+</sup> and Zn<sup>2+</sup> adsorption. We supposed that this phenomenon was due to the cationic exchange mechanism in the adsorption of Cd<sup>2+</sup> and Zn<sup>2+</sup> on the surface of MNHAP adsorbents. To demonstrate this supposition, we carried out some experiments to investigate whether Ca<sup>2+</sup> released in the solution after the completion of adsorption process. The results showed that the concentration of Ca<sup>2+</sup> in the solution increased remarkably after heavy metal adsorption compared with that one before heavy metal adsorption (from 0.3824 to 44.75 and 0.3835 to 31.29 mg L<sup>-1</sup> for Cd<sup>2+</sup> and Zn<sup>2+</sup> solutions respectively). Therefore,

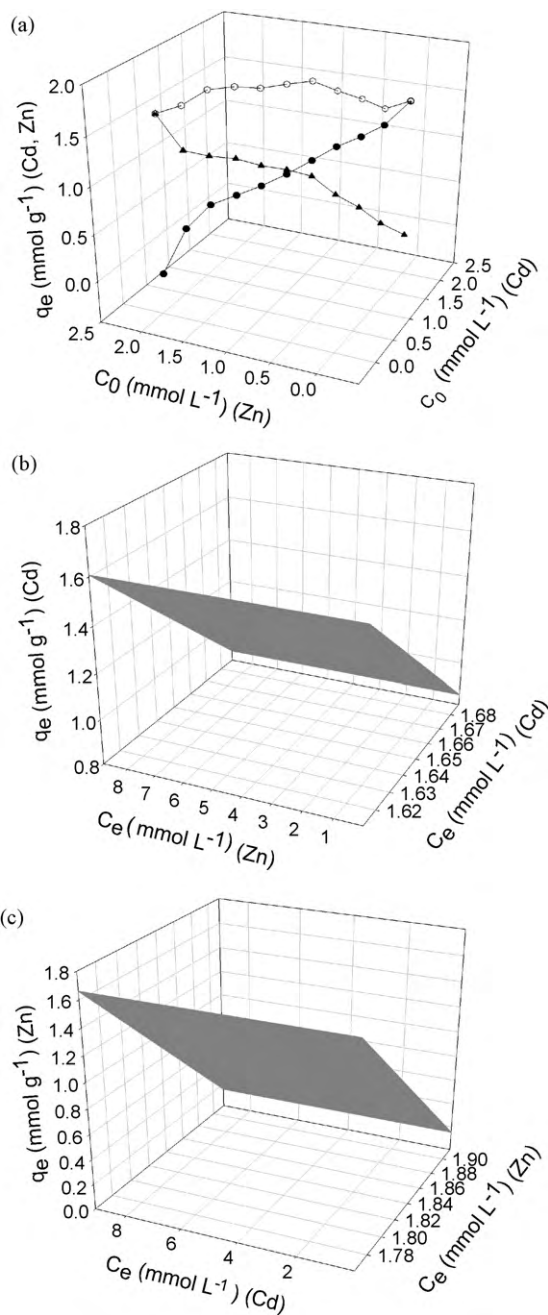


Fig. 8. The competitive adsorption behavior of Cd<sup>2+</sup> and Zn<sup>2+</sup>, (●) Cd<sup>2+</sup>; (▲) Zn<sup>2+</sup>; (○) Cd<sup>2+</sup> + Zn<sup>2+</sup>. (a) Effect of the fixed total initial concentration of Cd<sup>2+</sup> and Zn<sup>2+</sup> on the adsorption capacity of each metal ions; (b) the relationship between the adsorption capacity of Cd<sup>2+</sup> and the equilibrium concentrations of Cd<sup>2+</sup> and Zn<sup>2+</sup>; (c) the relationship between the adsorption capacity of Zn<sup>2+</sup> and the equilibrium concentrations of Cd<sup>2+</sup> and Zn<sup>2+</sup>.

it was concluded that there was a cation exchange mechanism in the adsorption process of Cd<sup>2+</sup> and Zn<sup>2+</sup>.

### 3.2.5. Competitive adsorption behavior of Cd<sup>2+</sup> and Zn<sup>2+</sup>

The relationship between the adsorption capacity and the initial concentration of Cd<sup>2+</sup> and Zn<sup>2+</sup> with the total concentration changeless was shown in Fig. 8a. It suggested that the equilibrium adsorption capacity of Cd<sup>2+</sup> and Zn<sup>2+</sup> ranged from 0.446 to 1.473 and 0.172 to 1.661 mmol g<sup>-1</sup> in the binary component systems, respectively, which were less than those in the single component solutions 1.664 mmol g<sup>-1</sup> for Cd<sup>2+</sup> and 1.838 mmol g<sup>-1</sup> for Zn<sup>2+</sup>. It indicated that one type of the metal ion present interfered with the

**Table 2**  
Desorption of Cd<sup>2+</sup> and Zn<sup>2+</sup> from loaded MNHAP adsorbents.

Eluants	Initial pH	Final pH		Desorbed (%)	
		Cd <sup>2+</sup>	Zn <sup>2+</sup>	Cd <sup>2+</sup>	Zn <sup>2+</sup>
EDTA (0.003 mol L <sup>-1</sup> )	2.54	5.26	5.06	66.2	67
HCl (0.01 mol L <sup>-1</sup> )	2.96	5.40	5.31	4.6	3.9
NaOH (0.01 mol L <sup>-1</sup> )	11.79	9.28	9.82	0.2	0.6
Ca(NO <sub>3</sub> ) <sub>2</sub> (0.01 mol L <sup>-1</sup> )	5.87	6.59	6.21	27	15.4

uptake of the other in the binary component system. The adsorption maximum of total adsorption was approximately constant. This fact indicates that Cd<sup>2+</sup> and Zn<sup>2+</sup> were adsorbed in the same sites.

The equilibrium adsorption capacity of Cd<sup>2+</sup> or Zn<sup>2+</sup> with the presence of Zn<sup>2+</sup> or Cd<sup>2+</sup> was shown in Fig. 8b and c, respectively. It was shown that, when both Cd<sup>2+</sup> and Zn<sup>2+</sup> were present in the solution together, some reduction of the Zn<sup>2+</sup> or Cd<sup>2+</sup> adsorbed could be observed. In Fig. 8b, the equilibrium adsorption capacity of Cd<sup>2+</sup> decreased from 1.607 to 0.848 mmol g<sup>-1</sup> with the initial concentration of Zn<sup>2+</sup> varying from 10<sup>-4</sup> to 10<sup>-2</sup> mol L<sup>-1</sup>. However, in Fig. 8c, when the initial concentration of Cd<sup>2+</sup> varied from 10<sup>-4</sup> to 10<sup>-2</sup> mol L<sup>-1</sup>, the equilibrium adsorption capacity of Zn<sup>2+</sup> decreased from 1.662 to 0.154 mmol g<sup>-1</sup>. Comparing with the equilibrium adsorption capacity in the single system, we could conclude that the interference of Cd<sup>2+</sup> with the Zn<sup>2+</sup> uptake was much more pronounced, since a distinct reduction of the Zn<sup>2+</sup> adsorbed was observed even at a relatively low Cd<sup>2+</sup> concentration. It confirmed that the MNHAP adsorbents had better affinity for cadmium ion than for zinc ion. The reason was due to the greater Langmuir constant of Cd<sup>2+</sup> than that of Zn<sup>2+</sup> in the adsorption process. Similar results were obtained by Corami et al. [39] when Cd<sup>2+</sup> was removed from multi-metal (Cd + Pb + Zn + Cu) solutions by sorption on hydroxyapatite.

### 3.3. Desorption experiment

The results of desorption studies were shown in Table 2. The amount of metal ions desorbed from EDTA solution was the maximum due to the formation of complex between EDTA and metal ions which possesses lower sorption affinity for MNHAP adsorbents [19]. Under acid conditions only trace amounts of metal ions desorbed can be observed and the amount of metal ions desorbed from alkaline solution was negligible. In addition, the amount of metal ions desorbed in the Ca(NO<sub>3</sub>)<sub>2</sub> solutions was 27% and 15.4% for Cd<sup>2+</sup> and Zn<sup>2+</sup>, respectively. This phenomenon may be attributed to the reversible process of cationic exchange between the MNHAP adsorbents surface and the solution. When the concentration of Ca<sup>2+</sup> in solution greatly exceeded that of MNHAP adsorbents, Ca<sup>2+</sup> was favored on the surface of MNHAP adsorbents resulting in the desorption of heavy metals which had been adsorbed on the adsorbents.

## 4. Conclusions

In this study, the adsorption potential of MNHAP for the removal of Cd<sup>2+</sup> and Zn<sup>2+</sup> from aqueous solutions was investigated. The effect of contact time, initial metal ions concentrations, pH, adsorbent dosage and competitive adsorption on the adsorption process was discussed. The following conclusions were obtained from the study.

- (1) Adsorption kinetic data were well fitted by the pseudo-second-order model with high interrelation coefficient ( $R^2 = 0.9999$ ) and adsorption isotherms were best described by the Langmuir model. The maximum adsorption capacity of Cd<sup>2+</sup> and Zn<sup>2+</sup> was 1.964 and 2.151 mmol g<sup>-1</sup> respectively. The optimal dosage of

adsorbent was 0.1 g L<sup>-1</sup>. The adsorption amount increased with increased pH ranging from 4 to 8.

- (2) In the binary component system, the adsorption maximum of total adsorption was approximately constant, but the MNHAP adsorbents had better affinity for cadmium ion than for zinc ion.
- (3) The most efficient eluant used for desorption of metal ions was EDTA with 66.2 and 67% of Cd<sup>2+</sup> and Zn<sup>2+</sup> released, respectively.
- (4) The most prominent advantage of prepared MNHAP adsorbents with paramagnetism and high specific surface area (142.5 m<sup>2</sup> g<sup>-1</sup>) was the separation convenience from aqueous solutions.

## Acknowledgements

The authors are grateful for the financial supports from National Natural science Foundation of China (50808070), the program for New Century Excellent Talents in University from the Ministry of Education of China (NCET-10-0328), the Postdoctoral Science Foundation of China (200902468, 20070410301), the Specialized Research Fund for the Doctoral Program of Higher Education (20070532059), the Program for Changjiang Scholars and Innovative Research Team in University (IRT0719), the National 863 High Technologies Research Foundation of China (2006AA06Z407), the Hunan Provincial Natural Science Foundation of China (08JJ4006), the Hunan Provincial Planned Science and Technology Project of China (2009SK4011) and the Xiangjiang Water Environmental Pollution Control Project subjected to the National Key Science and Technology Project for Water Environmental Pollution Control (2009ZX07212-001-02 and 2009ZX07212-001-06).

## Appendix A. Supplementary data

Supplementary data associated with this article can be found, in the online version, at doi:10.1016/j.cej.2010.05.049.

## References

- [1] P. Trivedi, L. Axe, Modeling Cd and Zn sorption to hydrous metal oxides, *Environ. Sci. Technol.* 34 (2000) 2215–2223.
- [2] W. Yantasee, C.L. Warner, T. Sangvanich, R.S. Addleman, T.G. Carter, R.J. Wiacek, G.E. Fryxell, C. Timchalk, M.G. Warner, Removal of heavy metals from aqueous systems with thiol functionalized superparamagnetic nanoparticles, *Environ. Sci. Technol.* 41 (2007) 5114–5119.
- [3] Z. Elouear, J. Bouzid, N. Boujelben, M. Feki, F. Jamoussi, A. Montiel, Heavy metal removal from aqueous solutions by activated phosphate rock, *J. Hazard. Mater.* 156 (2008) 412–420.
- [4] G. Crini, Recent developments in polysaccharide-based materials used as adsorbents in wastewater treatment, *Prog. Polym. Sci.* 30 (2005) 38–70.
- [5] G. Crini, Non-conventional low-cost adsorbents for dye removal: a review, *Bioresour. Technol.* 97 (2006) 1061–1085.
- [6] R. Apiratikul, P. Pavasant, Sorption of Cu<sup>2+</sup>, Cd<sup>2+</sup>, and Pb<sup>2+</sup> using modified zeolite from coal fly ash, *Chem. Eng. J.* 144 (2008) 245–258.
- [7] S.K. Pitcher, R.C.T. Slade, N.I. Ward, Heavy metal removal from motorway stormwater using zeolites, *Sci. Total Environ.* 334–335 (2004) 161–166.
- [8] K.G. Bhattacharyya, S.S. Gupta, Influence of acid activation on adsorption of Ni (II) and Cu (II) on kaolinite and montmorillonite: Kinetic and thermodynamic study, *Chem. Eng. J.* 136 (2008) 1–13.
- [9] P.X. Wu, W.M. Wu, S.Z. Li, N. Xing, N.W. Zhu, P. Li, J.H. Wu, C. Yang, Z. Dang, Removal of Cd<sup>2+</sup> from aqueous solution by adsorption using Fe-montmorillonite, *J. Hazard. Mater.* 169 (2009) 824–830.
- [10] Y. Huang, X.Y. Ma, G.Z. Liang, H.X. Yan, Adsorption of phenol with modified rectorite from aqueous solution, *Chem. Eng. J.* 141 (2008) 1–8.
- [11] Y. Huang, X.Y. Ma, G.Z. Liang, Y.X. Yan, S.H. Wang, Adsorption behavior of Cr (VI) on organic-modified rectorite, *Chem. Eng. J.* 138 (2008) 187–193.
- [12] M.A. Al-Ghouti, M.A.M. Khraisheh, M. Tutuji, Flow injection potentiometric stripping analysis for study of adsorption of heavy metal ions onto modified diatomite, *Chem. Eng. J.* 104 (2004) 83–91.
- [13] M. Sljivic, I. Smiciklas, S. Pejanovic, I. Plecas, Comparative study of Cu<sup>2+</sup> adsorption on a zeolite, a clay, and a diatomite from Serbia, *Appl. Clay Sci.* 43 (2009) 33–40.
- [14] F.G. Simon, V. Biermann, B. Peplinski, Uranium removal from groundwater using hydroxyapatite, *Appl. Geochem.* 23 (2008) 2137–2145.

- [15] C.S. Sundaram, N. Viswanathan, S. Meenakshi, Defluoridation chemistry of synthetic hydroxyapatite at nano scale: equilibrium and kinetic studies, *J. Hazard. Mater.* 155 (2008) 206–215.
- [16] A. Krestou, A. Xenidis, D. Panias, Mechanism of aqueous uranium (VI) uptake by hydroxyapatite, *Miner. Eng.* 17 (2004) 373–381.
- [17] M. Srinivasan, C. Ferraris, T. White, Cadmium and lead ion capture with three dimensionally ordered macroporous hydroxyapatite, *Environ. Sci. Technol.* 40 (2006) 7054–7059.
- [18] Y.P. Xu, F.W. Schwartz, S.J. Traina, Sorption of  $Zn^{2+}$  and  $Cd^{2+}$  on hydroxyapatite surfaces, *Environ. Sci. Technol.* 28 (1994) 1472–1480.
- [19] Y.J. Wang, J.H. Chen, Y.X. Cui, S.Q. Wang, D.M. Zhou, Effects of low-molecular-weight organic acids on Cu (II) adsorption onto hydroxyapatite nanoparticles, *J. Hazard. Mater.* 162 (2009) 1135–1140.
- [20] A. Dybowska, D.A.C. Manning, M.J. Collins, T. Wess, S. Woodgate, E. Valsami-Jones, An evaluation of the reactivity of synthetic and natural apatites in the presence of aqueous metals, *Sci. Total Environ.* 407 (2009) 2953–2965.
- [21] A. Corami, S. Mignardi, V. Ferrini, Copper and zinc decontamination from single- and binary-metal solutions using hydroxyapatite, *J. Hazard. Mater.* 146 (2007) 164–170.
- [22] I. Smiciklas, A. Onjia, S. Raicevic, D. Janackovic, M. Mitric, Factors influencing the removal of divalent cations by hydroxyapatite, *J. Hazard. Mater.* 152 (2008) 876–884.
- [23] J.A. Gomez del Rio, P.J. Morando, D.S. Cicerone, Natural materials for treatment of industrial effluents: comparative study of the retention of Cd, Zn and Co by calcite and hydroxyapatite. Part I: batch experiments, *J. Environ. Manage.* 71 (2004) 169–177.
- [24] Z.H. Ai, Y. Cheng, L.Z. Zhang, J.R. Qiu, Efficient removal of Cr (VI) from aqueous solution with Fe@Fe<sub>2</sub>O<sub>3</sub> core-shell nanowires, *Environ. Sci. Technol.* 42 (2008) 6955–6960.
- [25] S. Pal, E.C. Alocilja, Electrically active polyaniline coated magnetic (EAPM) nanoparticle as novel transducer in biosensor for detection of *Bacillus anthracis* spores in food samples, *Biosens. Bioelectron.* 24 (2009) 1437–1444.
- [26] V. Rocher, J.M. Siaugue, V. Cabuil, A. Bee, Removal of organic dyes by magnetic alginate beads, *Water Res.* 42 (2008) 1290–1298.
- [27] J.L. Gong, B. Wang, G.M. Zeng, C.P. Yang, C.G. Niu, Q.Y. Niu, W.J. Zhou, Y. Liang, Removal of cationic dyes from aqueous solution using magnetic multi-wall carbon nanotube nanocomposite as adsorbent, *J. Hazard. Mater.* 164 (2009) 1517–1522.
- [28] G.S. Zhang, J.H. Qu, H.J. Liu, R.P. Liu, R.C. Wu, Preparation and evaluation of a novel Fe–Mn binary oxide adsorbent for effective arsenite removal, *Water Res.* 41 (2007) 1921–1928.
- [29] G.S. Zhang, H.J. Liu, R.P. Liu, J.H. Qu, Removal of phosphate from water by a Fe–Mn binary oxide adsorbent, *J. Colloid Interface Sci.* 335 (2009) 168–174.
- [30] K. Mori, S. Kanai, T. Hara, T. Mizugaki, K. Ebitani, K. Jitsukawa, K. Kaneda, Development of ruthenium-hydroxyapatite-encapsulated superparamagnetic  $\gamma$ -Fe<sub>2</sub>O<sub>3</sub> nanocrystallites as an efficient oxidation catalyst by molecular oxygen, *Chem. Mater.* 19 (2007) 1249–1256.
- [31] K.L. Lin, J.Y. Pan, Y.W. Chen, R.M. Cheng, X.C. Xu, Study the adsorption of phenol from aqueous solution on hydroxyapatite nanopowders, *J. Hazard. Mater.* 161 (2009) 231–240.
- [32] I. Smiciklas, S. Dimovic, I. Plecas, M. Mitric, Removal of Co<sup>2+</sup> from aqueous solutions by hydroxyapatite, *Water Res.* 40 (2006) 2267–2274.
- [33] R.H. Zhu, R.B. Yu, J.X. Yao, D. Mao, C.J. Xing, D. Wang, Removal of Cd<sup>2+</sup> from aqueous solutions by hydroxyapatite, *Catal. Today* 139 (2008) 94–99.
- [34] Z.Y. Ma, Y.P. Guan, H.Z. Liu, Synthesis and characterization of micron-sized monodisperse superparamagnetic polymer particles with amino groups, *J. Polym. Sci. Polym. Chem.* 43 (2005) 3433–3439.
- [35] K. Chojnacka, Equilibrium and kinetic modeling of chromium (III) sorption by animal bones, *Chemosphere* 59 (2005) 315–320.
- [36] C.W. Cheung, J.F. Porter, G. Mckay, Sorption kinetic analysis for the removal of cadmium ions from effluents using bone char, *Water Res.* 35 (2001) 605–612.
- [37] P.K. Chaturvedi, C.S. Seth, V. Misra, Sorption kinetics and leachability of heavy metal from the contaminated soil amended with immobilizing agent (humus soil and hydroxyapatite), *Chemosphere* 64 (2006) 1109–1114.
- [38] S. Saxena, M. Prasad, S.F. D'Souza, Radionuclide sorption onto low-cost mineral adsorbent, *Ind. Eng. Chem. Res.* 45 (2006) 9122–9128.
- [39] A. Corami, S. Mignardi, V. Ferrini, Cadmium removal from single- and multi-metal (Cd + Pb + Zn + Cu) solutions by sorption on hydroxyapatite, *J. Colloid Interface Sci.* 317 (2008) 402–408.